

VU Research Portal

Linear dichroism of CdSe nanodots: Large anisotropy of the band-gap absorption induced by ground-state dipole moments

van Mourik, F.; Giraud, G.; Tonti, D.; Chergui, M.; van der Zwan, G.

published in

Physical Review B. Condensed Matter and Materials Physics
2008

DOI (link to publisher)

[10.1103/PhysRevB.77.165303](https://doi.org/10.1103/PhysRevB.77.165303)

document version

Publisher's PDF, also known as Version of record

[Link to publication in VU Research Portal](#)

citation for published version (APA)

van Mourik, F., Giraud, G., Tonti, D., Chergui, M., & van der Zwan, G. (2008). Linear dichroism of CdSe nanodots: Large anisotropy of the band-gap absorption induced by ground-state dipole moments. *Physical Review B. Condensed Matter and Materials Physics*, 77(1, Pages = 165303,), 165303.
<https://doi.org/10.1103/PhysRevB.77.165303>

General rights

Copyright and moral rights for the publications made accessible in the public portal are retained by the authors and/or other copyright owners and it is a condition of accessing publications that users recognise and abide by the legal requirements associated with these rights.

- Users may download and print one copy of any publication from the public portal for the purpose of private study or research.
- You may not further distribute the material or use it for any profit-making activity or commercial gain
- You may freely distribute the URL identifying the publication in the public portal ?

Take down policy

If you believe that this document breaches copyright please contact us providing details, and we will remove access to the work immediately and investigate your claim.

E-mail address:

vuresearchportal.ub@vu.nl

Linear dichroism of CdSe nanodots: Large anisotropy of the band-gap absorption induced by ground-state dipole moments

Frank van Mourik, Gérard Giraud,^{*} Dino Tonti,[†] and Majed Chergui

Ecole Polytechnique Fédérale de Lausanne, Laboratory of Ultrafast Spectroscopy, Institut de Sciences et Ingénierie Chimiques, FSB-BSP, CH-1015 Lausanne-Dorigny, Switzerland

Gert van der Zwan

Laser Centre VU, Analytical Chemistry and Applied Spectroscopy, Faculty of Sciences, Vrije Universiteit Amsterdam, de Boelelaan 1083, 1081 HV Amsterdam, The Netherlands

(Received 24 October 2007; revised manuscript received 13 February 2008; published 2 April 2008)

We measured the electric field induced linear dichroism for a wide range of sizes of CdSe nanocrystals. Large ground-state dipole moments were observed, especially for the smallest crystals. In these, we found a very large anisotropy of the absorption and most of the dipole strength is along the direction of the ground-state dipole moment. For the anisotropy, we propose a mechanism for intensity borrowing from intraband transitions, induced by the field of the ground-state dipole moment.

DOI: [10.1103/PhysRevB.77.165303](https://doi.org/10.1103/PhysRevB.77.165303)

PACS number(s): 78.67.Hc, 73.22.-f, 78.20.Jq

I. INTRODUCTION

Nanocrystals of CdSe can be prepared by wet chemistry with good yields, well defined shapes, and narrow size distributions.^{1,2} The strong confinement of the electron wave function in these particles makes it possible to tune their optical properties, with many applications in biology and optoelectronics. A large number of theoretical and experimental studies have addressed the electronic structure of CdSe nanocrystals, leading to rather detailed models³ for their spectroscopy. However, several experiments strongly challenge the current models. The most problematic are the observations of parity violation, as deduced from two-photon excitation experiments.⁴ Moreover, dielectric spectroscopy⁵ and transient electric birefringence measurements⁶ have revealed large ground-state dipole moments in CdSe nanodots and rods. The origin of the dipole moments is not entirely clear; theoretical studies predict a dipole moment for CdSe nanocrystals due to deviations from the wurtzite structure.⁷ However, the predicted scaling of the dipole moment with the volume of the particles was not observed for dots.⁴ Also, for cubic crystal structures, large dipole moments have been reported,⁸ which could be due to truncation effects of the nanocrystals.^{9,10} Here, we report on electric field induced linear dichroism (LD) measurements. Contrary to dielectric dispersion and birefringence experiments, LD is a resonant technique, which allows us to obtain both the dipole moment of the particles and the orientation of the optical transitions with respect to the dipole moment.

II. EXPERIMENT

For the LD measurements, a cell with vertical electrodes spaced 3 mm apart and an optical path length of 10 mm was constructed. Measuring light was horizontally polarized. The field was generated by a function generator running at 1 kHz and amplified in a Trek 10B amplifier. The signal was detected (by an Avalanche Photodiode) with a lock-in amplifier at the second harmonic of the field frequency. The lock-in

amplifier measures the difference in transmission between field on and field off, corresponding to the difference between partially aligned and isotropic transmissions of the sample. For all samples, a field strength of 11.8 kV/cm was used. Measurements were performed on commercially available samples (Evident Technologies) and similar homemade samples. The samples were diluted in spectroscopic grade toluene and sonicated before the experiments. In the following, we presume the dipole moment of the particles to be along the c axis of the particles, and we treat the particles as cylindrically symmetric around the c axis, i.e., the only parameter for the distribution is the angle between dipole moment and electric field. Since the rotational diffusion time of the particles is 3 orders of magnitude shorter than the period of the field, we presume that the orientational distribution of the particles is, at all times, well approximated by a Boltzmann distribution, as in

$$P(\theta, E) d\theta = \frac{\sin(\theta) \exp\left(\frac{\cos(\theta) E \mu}{k_B T}\right)}{\int_0^\pi \sin(\alpha) \exp\left(\frac{\cos(\alpha) E \mu}{k_B T}\right) d\alpha} d\theta. \quad (1)$$

Here, E is the field, μ is the dipole moment, and θ is the angle between the dipole moment and the field. The LD signal is defined as

$$\frac{A_E - A_0}{A_{\text{iso}}} = (3 \cos^2 \chi - 1) \frac{\int_0^\pi [P(\theta, E) - P(\theta, 0)] \cos^2 \theta d\theta}{\int_0^\pi P(\theta, 0) \cos^2 \theta d\theta}, \quad (2)$$

where A_E and A_0 are the absorption of the sample with the field on and off, respectively, A_{iso} is the isotropic absorption spectrum (measured independently), and χ is the angle between the transition dipole moment and the c axis of the crystal. If we ignore dielectric effects, for a particle with a 100 D dipole moment in an 11.8 kV/cm field, the LD/A_{iso}

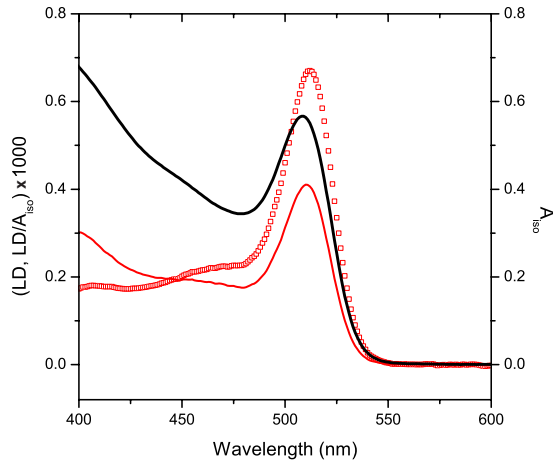


FIG. 1. (Color online) Electric field linear dichroism (solid red/gray) and absorption spectra (black) of 2.4 nm diameter CdSe nanocrystals (from Evident Technologies). The dotted curve is the LD/A_{iso} .

value would be 1.2×10^{-3} for a transition polarized parallel to the dipole moment.

III. RESULTS

The most common model³ for the band edge exciton states of CdSe nanocrystals predicts a forbidden lowest energy transition (± 2), with the first allowed transition $\pm 1^L$ about 10 meV higher in energy. The next transition is the forbidden 0^L , followed by the allowed $\pm 1^U$ and 0^U transitions. Of these transitions, only the 0^L and 0^U are polarized along the c axis of the particle; all other transitions are degenerate and polarized perpendicular to the axis. The dipole strength of the transitions is such that it is isotropically distributed over the x, y, z directions when integrated over the band gap.

Figure 1 shows a typical LD ($A_E - A_0$) spectrum for one of the smaller dot sizes, together with the isotropic absorption spectrum and the LD/A_{iso} spectrum. The signal is positive over the band edge region and beyond, which indicates that the band gap absorption is dominated by the transitions oriented or polarized along the axis of orientation. This is an obvious deviation from theory, which predicts that the band gap region has an isotropic oscillator strength, i.e., the integrated LD signal should be zero. Instead, we find that the absorption along the c axis has a significantly larger dipole strength than the perpendicular transitions.

In Fig. 2, we model the absorption and LD spectra based on the theoretical positions and dipole strengths of the three optically allowed transitions in the band gap region.³ Not surprisingly, the band gap absorption is very easily simulated with this parameter set (upper panel in Fig. 2). However, the predicted LD spectrum is very far off from the experimental spectrum. To get a better correspondence between theory and experiment, the axial absorption bands (0^L and 0^U) need to have a significantly higher dipole strength than that of the perpendicular transitions. Moreover, since the LD and LD/A_{iso} spectra peak on the red side of the band, the axial

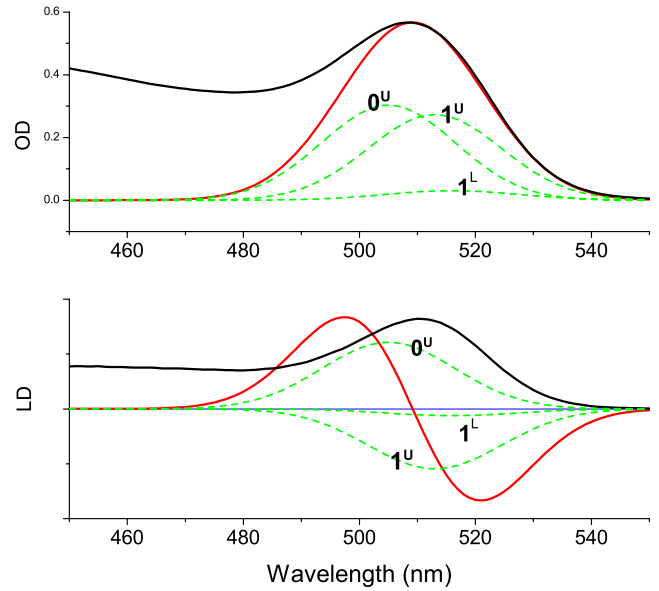


FIG. 2. (Color online) Simulation of the absorption (upper panel) and electric field induced LD spectra (lower panel) of Fig. 1. The relative positions and dipole strength of the three bands used to describe the OD spectrum were taken from Ref. 3 and shifted in parallel to fit the low energy side of the band-gap absorption. Relative positions of the transitions are 0 meV ($\pm 1^L$), 37 meV ($\pm 1^U$), and 51 meV (0^U), with relative dipole strengths scaling as 0.1: 0.9: 1.0. All of the bands were given a Gaussian width of 27 nm. In the lower panel, the same bands were used to calculate the LD spectrum (solid red/gray curve). The black curve is the experimental LD spectrum.

transitions need to be redshifted significantly. We estimate that the axial transitions must be at least three times stronger than the perpendicular transitions; otherwise, negative contributions would be visible in the red or blue side of the spectrum, which is clearly not the case. Since the spectra of this sample lack structure, we have not attempted a free fit of the data. Without a deconvolution of the bands underlying the band gap, we cannot arrive at an absolute value for the LD/A_{iso} value of the individual transitions. This requires an accurate model that describes the fine structure of the band gap. Given the obvious discrepancies between experiment and theory, we cannot directly apply a model. However, for the small particles, the domination of the axial absorption is large enough, such that the estimated dipole moment is not very dependent on the exact increase in dipole strength, and we can estimate a ground-state dipole moment of 80–110 D (the higher values are based on a correction for the overlapping bands, with a fourfold enhancement of the 0^U transition). Note that the dipole field not only affects the strengths of the transitions, but also shifts the levels. As a result, a heterogeneity in the magnitude of the dipole moment would lead to a broadening of the band gap transition, possibly with a comparable magnitude to that of broadening due to the distribution in size. This could provide an explanation for the relatively redshifted LD band of the band gap, since the position within the inhomogeneous band would be correlated with the dipole moment. Therefore, the contribution of a par-

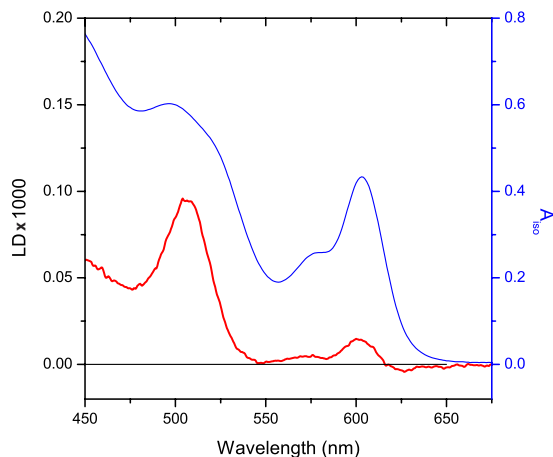


FIG. 3. (Color online) Electric field linear dichroism (red, lower curve) and absorption spectra (blue, upper curve) of 4.7 nm diameter CdSe nanocrystals from Evident Technologies.

ticle to the LD spectrum would be weighted by the square of its ground-state dipole moment, resulting in a redshifted LD spectrum. Figure 3 shows a LD spectrum typical of larger nanocrystals. Note that the magnitude of the LD signal in the band gap region is more than an order of magnitude smaller than that in Fig. 1. We observed a negative LD signal on the red side of the band for particle sizes of ≥ 3.7 nm diameter. The appearance of this feature is in accordance with the theoretical model, which predicts a redistribution of the dipole strength from the $\pm 1^U$ to the $\pm 1^L$ transitions³ when going from small to large particles. In Fig. 4, we model the results with the predictions of theory. Again, the result is not very good for the LD spectrum (middle panel). However, a minor change in the dipole strength (10%) in combination with a redshift by 4 nm of the 0^U band generates a LD spectrum that resembles the experimental spectrum (lower panel in Fig. 4). We did not attempt to find a combination of bands that would fit both the absorption and LD spectra. As discussed above, if the ground-state dipole moment is not the same for all particles, the LD spectrum will be biased toward a redshifted subpopulation of the particles. Therefore, the bands used to simulate the isotropic absorption spectrum in the top panel of Fig. 4 need not be the same ones that work for the description of the LD spectrum in the bottom panel. The main conclusion that we want to draw from this simulation is that, again, the axial dipole strength needs to be slightly enhanced and redshifted. The strongly overlapping contributions in the band gap area make it harder to arrive at an estimate of the degree of orientation of the particles. Fortunately, this sample does show a strong LD/A_{iso} signal for a higher energy transition (probably the $1P_{3/2}1P_e$ transition), peaking at about 500 nm, which corresponds to a dipole moment of at least 37 D (value obtained if the observed band would be a transition, purely polarized along the axis of the crystal, without interfering negative contributions). An estimate based on the simulation of Fig. 4 leads to a value of 48 D for the ground-state dipole moment. The smaller dipole moment (in comparison with the smaller particles) in combination with the larger diameter of these particles should result in an internal

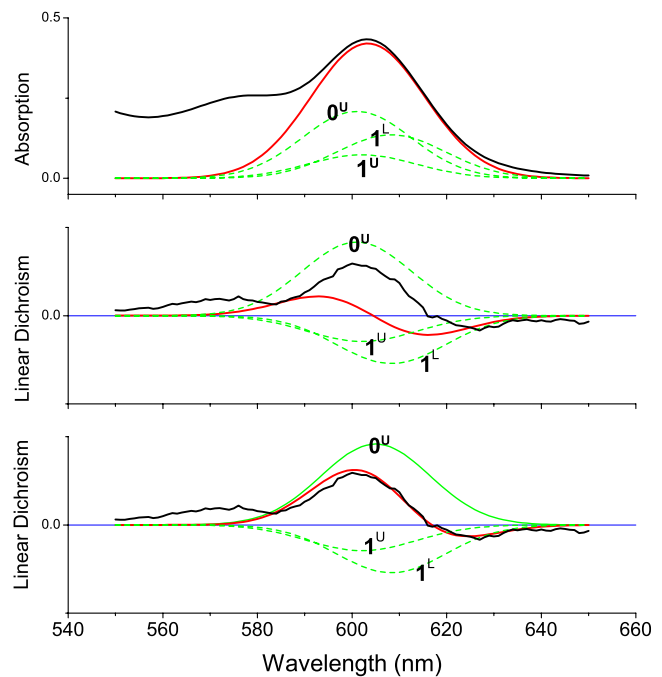


FIG. 4. (Color online) Simulation of the absorption and electric field linear dichroism spectra of 4.7 nm diameter CdSe nanocrystals. The relative positions and dipole strength of the three bands (dashed green) used to describe the OD spectrum were taken from Ref. 3 and shifted in parallel to fit the low energy side of the band-gap absorption. Relative positions of the transitions are 0 meV ($\pm 1^L$), 21 meV ($\pm 1^U$), and 25 meV (0^U), with relative dipole strengths scaling as 0.65: 0.35: 1. All of the bands were given a Gaussian width of 27 nm. The full green curve in the lower panel is the shifted 0^U , enhanced by 10%.

field that is about four times smaller than the field in the small particles. This explains the smaller deviation from theory, which is observed for the larger particles.

The change in dipole strength of the axial absorption of the smaller particle is of such a magnitude that it should also affect the isotropic spectrum. In this respect, it is good to look at the relative strength of the band gap transitions as compared to the size-independent continuum absorption at short wavelengths. As reported in Refs. 11 and 12, the absorption at 350 nm is more or less representative of the total amount of CdSe in the sample, independent of particle size. In Fig. 5, we plotted the isotropic absorption spectra of the preparations we used in this study, with each spectrum normalized to its absorption at 350 nm. When presented like this, the relative contribution of the band gap transition increases when going from large to small particles. Actually, the trend observed in Fig. 5 correlates well with the two LD spectra shown here. The proposed fourfold increase in the axial absorption needed to explain the LD spectrum of the small particle would result in a doubling of its isotropic absorption, which is actually what is observed in Fig. 5. Therefore, the change in relative intensity of the band gap transition as a function of size could be completely due to the observed increase in the axial absorption. The observed trend also justifies our choice to model the LD spectra by an increase in the axial absorption, whereas a decrease in the per-

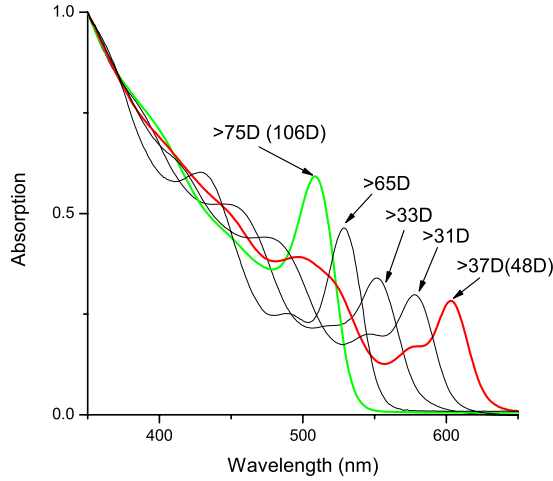


FIG. 5. (Color online) Absorption spectra, normalized at 350 nm, of the CdSe nanocrystals used in our LD experiments. The red/dark gray and green/light gray curves correspond to the experiments shown in Figs. 1 and 3. Indicated are the values obtained for the ground-state dipole moment without and with deconvolution (between brackets, as described in the text).

pendicular dipole strength would have also explained the LD results. The estimates of the ground-state dipole moments given in Fig. 5 correspond to the value deduced from the maximal value of the LD/ A_{iso} spectrum, without a correction for compensating negative contributions.

The permanent dipole moment inherent to CdSe nanoparticles, which causes it to orient in an external field, is also the cause of an internal field that can perturb the excitonic structure. A 100 D dipole moment, due to an asymmetric charge distribution within the particle, gives rise to a field of ~ 3 MV/cm, which can have a significant interaction with the transition moments of the system. However, the enhanced axial dipole strength is not easily explained by the interaction of an isolated transition dipole moment with the field. For a two-level system, the effect of an electric field would be to reduce the dipole strength of the transition.¹³ Therefore, the field induced mixing of other transitions also needs to be taken into account, and a crucial role is played by the intraband transitions.

In the following, we present a four-level model that rationalizes the observed behavior. An exciton consists of an electron in the conduction band, and a hole in the valence band, subject to the boundary condition that the wave function vanishes at the surface of the (spherical) particle. A basis set is usually chosen as eigenfunctions of the total angular momentum operator, since it commutes with the Hamiltonian of the system. The electron and hole wave functions thus become the product of an underlying Bloch function and an envelope function. The Bloch functions reflect the electronic properties of the bands, making the electron behave as a spin 1/2 particle and the hole as a spin 3/2 particle. Eigenfunctions can then be written as $|lff_z\rangle$, where l is the angular momentum of the envelope function and f and f_z are the total angular momentum and its z projection, respectively. A general excitonic state can thus be written as the product of an electron state and a hole state $|lff_z\rangle|LFF_z\rangle$. Usually, only the

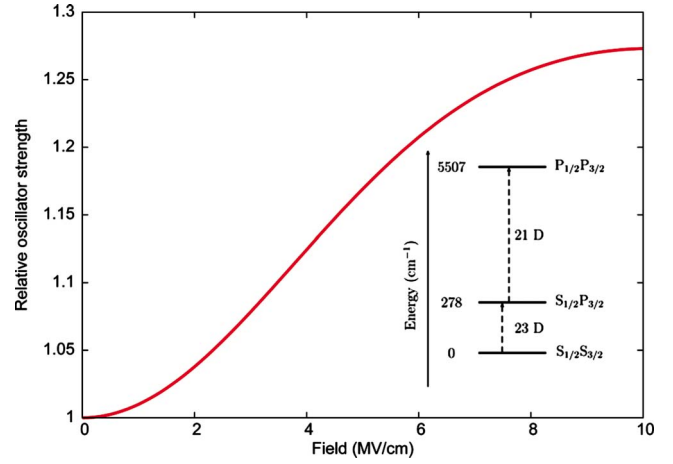


FIG. 6. (Color online) Relative dipole strength of the axial transitions ($0^U + 0^L$) as a function of the “internal field.” The inset shows the possible intraband transitions starting from one of the states comprising 0^U . Energies and transition dipole moments (in D) are all for a particle of 2.5 nm radius. Energies are relative to the lowest optically excited state. The highest state is also optically allowed. The states indicated are all eightfold degenerate, and for the ones that have a transition moment in the z direction, the magnitudes are given.

lowest exciton band $l=0$, $L=0$ is considered for the optical transitions. Initially, none of the states have a permanent dipole moment. We assume the internal field to be in the z direction, which is the same direction as the crystal field. However, in contrast to the electron–hole interaction and the crystal field splitting, the electric field breaks the inversion symmetry, changing the selection rules for transitions to these states. The lowest excitonic state of relevance that is optically allowed and has a transition moment in the z direction is the transition to¹⁴

$$|0^U\rangle = \frac{1}{\sqrt{2}} \left[-i |0 \frac{1}{2} \frac{1}{2}\rangle |0 \frac{3}{2} - \frac{1}{2}\rangle + |0 \frac{1}{2} - \frac{1}{2}\rangle |0 \frac{3}{2} \frac{1}{2}\rangle \right]. \quad (3)$$

The orthogonal linear combination of the two states on the right hand side is the optically forbidden $|0^L\rangle$ state. From this state, intraband transitions with a transition dipole moment in the z direction are possible to a number of states. In principle, intraband transitions are possible from S to P envelope states for both the hole and the electron, which gives a total number of 128 possible states. A full description of the intraband transitions and the effects of an electric field on them will be given in a separate paper. Here, we confine ourselves to what appears to be the dominant effect. In Fig. 6, we show a small subset of states accessible from one of the states of Eq. (3). From $|0 \frac{1}{2} \frac{1}{2}\rangle |0 \frac{3}{2} - \frac{1}{2}\rangle$, an intraband transition is possible to $|0 \frac{1}{2} \frac{1}{2}\rangle |1 \frac{3}{2} - \frac{1}{2}\rangle$, and another intraband transition to the, again, optically allowed state $|1 \frac{1}{2} \frac{1}{2}\rangle |1 \frac{3}{2} - \frac{1}{2}\rangle$. We concentrate on these states since the first two are close lying in energy and have a large transition dipole moment in the z direction between them. Energy differences and transition dipole moments were calculated for CdSe by using the Luttinger parameter set.¹⁵ The electric field acts on the transition mo-

ments between the states. For the optical transitions, these are calculated in the usual way.¹⁴ For the intraband transitions, we let the dipole operator,

$$\hat{\mu} = e\mathbf{r}_h - e\mathbf{r}_e, \quad (4)$$

where \mathbf{r}_h is the hole position and \mathbf{r}_e is the electron position, act between the states. The dependence of the Hamiltonian on the internal electric field is then given by $-\hat{\mu} \cdot \mathbf{E}$. The external electric field, which orients the dipoles, can be neglected in these calculations, since it is generally at least an order of magnitude weaker than the internal field within the nanodot.

The effect of an electric field on this subsystem can be obtained by diagonalizing the resulting 4×4 Hamiltonian, which comprises the ground state, the optically allowed states $S_{1/2}S_{3/2}$ and $P_{1/2}P_{3/2}$, and the intermediate state $S_{1/2}P_{3/2}$, for a given electric field strength. Briefly stated, the main effects are the following: a considerable mixing of the two low lying states, which make them now both optically allowed; the states themselves acquire dipole moments; and the previously optically forbidden 0^L transition now also becomes optically allowed. Since the difference in energy between these states is smaller than the bandwidth, all of the states contribute to the oscillator strength of the lowest transition, which can then increase in value. Figure 6 shows how this model predicts an increase in the axial dipole strength by about 5% for an internal field of 3 MV/cm, i.e., the right order of magnitude for the data presented in Figs. 3 and 4. The four-level model presented here is the minimal model to predict field induced dipole-strength enhancements. The model is not really sufficient for a quantitative description of the stronger effects occurring in the smaller particles. Obviously, the stronger the field, the more the states and transitions need to be taken into account.

IV. DISCUSSION

Our results show that care has to be taken when extrapolating experimental data obtained on nanocrystals of a certain size to other sizes. The spectroscopy of the smaller crystals is very different from that of the larger ones. The size dependence and magnitude of the dipole moments reported here differ from those deduced from dielectric spectroscopy experiments.⁵ We do not know where the discrepancy comes from, but we note that, contrary to what is the case for the dielectric spectroscopy experiments,⁵ the interpretation of our LD experiment does not require knowledge of the absolute concentration of particles, which eliminates a possible source of error. Aggregation could lead to larger LD signals if the aggregate has a larger dipole moment than the individual particle. However, sonication and tenfold dilution of the sample did not have an effect on the spectra of the particles, making it unlikely that aggregation plays a role. Two mechanisms have been proposed for the large ground-state dipole moments in semiconductor nanocrystals. For wurtzite CdSe, it was suggested that a deviation from the ideal lattice structure, leading to a slightly polar lattice, could give rise to a dipole moment that scales with the volume of the particle.⁷ For zinc blende crystals, this explanation does not work and,

in order to explain the fact that also zinc blende crystals exhibit dipole moments, asymmetry in the termination of the crystals has to play a role.⁹ Because of the large difference in electronegativity of Cd and Se, the surface atoms carry a partial charge, which is compensated by the neighboring atoms; this could be envisaged as a surface that contains a finite number of dipoles. An imbalance between the number of dipoles pointing to a certain direction can then lead to an overall dipole moment. For PbSe, it was proposed that this mechanism can have a preferential direction with respect to the crystal axis and that the dipole moments play a role in the assembly of nanowires.¹⁰ Note that, especially for small crystals, the attraction between dipoles on opposite sides of the crystal, pointing to the same direction, can stabilize particles with a large dipole moment. This could be an explanation for the counterintuitive trend in the magnitude of the dipole moment that we observe. Both the absence of a scaling of the ground-state dipole moment with the volume, the particle, and the magnitude of the dipole moments indicate that the truncation mechanism, as proposed by Shanbhag and Kotov, could be the relevant one for the small particles. The alternative model of Nann and Schneider⁷ predicted a dipole moment of 1.27 D nm^{-3} . For the smallest particles in our study, this corresponds to a dipole moment of about 10 D, which is about an order of magnitude less than what we observe. However, this small dipole moment resulting from the polar lattice could play a coordinating role during the assembly of the particles. Our results seem to indicate that the ground-state dipole moment is along the hexagonal axis. Given the stochastic nature of the truncation mechanism, this would not be very likely without some form of coordination.

For the large particle that we measured, the model of Nann and Schneider predicted a dipole moment of 70 D, which is close to what we estimated (48 D) from our experiment. The above mentioned stabilization due to the attraction of dipole moments on opposite sides of a crystal diminishes for larger crystals, and obviously even more so for rod-shaped particles. Therefore, it is reasonable to assume that for large dots and rods, the dipole moments are caused by the polarity of the lattice, as suggested by Nann and Schneider.⁷

For the smaller particles, the magnitude of the local field of the dipole moment could be large enough to supersede the crystal field splitting in determining the spectroscopy of the nanocrystals. Indeed, recent photoluminescence and fluorescence line narrowing studies on CdSe nanodots having a wurtzite or a zinc blende structure show that their spectral features are identical. To explain this, we suggest that the ground-state dipole moment takes over the role of the crystal field in zinc blende crystals.¹⁶ Although in this work we only addressed the effects of the dipole moment on the ground-state absorption spectrum, we would like to stress the impact on the charge recombination dynamics in these particles. As we have demonstrated, the axial absorption bands are mixed states, which should open up additional relaxation pathways for the band edge exciton. This could be an explanation for the fact that the predicted phonon bottleneck^{17,18} has never really been demonstrated in a convincing way. Also in PbSe nanocrystals, where due to strong confinement phonon bottleneck effects were expected to be prominent, relaxation processes occur on the same fast time scale as in CdSe

nanocrystals.^{19,20} This is not so surprising since for PbSe nanocrystals large dipole moments have also been reported.¹⁰ The mixing of states in the band gap was already deduced from two-photon excitation experiments,⁴ but the implications have largely been ignored. This is perhaps due to the “bipolar” nature of the dots; i.e., they really show a wide variety of dynamics: due to the strong mixing of states in the axial absorption bands, intraband relaxation processes can be extremely fast.^{20,21} On the other hand, in low temperature experiments, an almost atomlike behavior is observed. This can be understood since the lowest states of the exciton

manifold ($\pm 1^L$ and ± 2), which are responsible for the low temperature behavior, are polarized perpendicular to the axis and, thus, do not interact with the field of the ground-state dipole moment.

ACKNOWLEDGMENTS

This work was supported by the Swiss National Science Foundation (Project No. 200020-105333) and by the NCCR Quantum Photonics program.

*Present address: COSMIC, The University of Edinburgh, Mayfield Road, Edinburgh EH9 3JZ, UK.

†Present address: Instituto de Ciencia de Materiales de Madrid, CSIC, Cantoblanco ES-28049 Madrid, Spain.

¹C. Murray, C. Kagan, and M. Bawendi, *Annu. Rev. Mater. Sci.* **30**, 545 (2000).

²M. Mohamed, D. Tonti, A. Al-Salman, A. Chemsiddine, and M. Chergui, *J. Phys. Chem. B* **109**, 10533 (2005).

³A. L. Efros and M. Rosen, *Annu. Rev. Mater. Sci.* **30**, 475 (2000).

⁴M. E. Schmidt, S. A. Blanton, M. A. Hines, and P. Guyot-Sionnest, *J. Chem. Phys.* **106**, 5254 (1997).

⁵S. A. Blanton, R. L. Leheny, M. A. Hines, and P. Guyot-Sionnest, *Phys. Rev. Lett.* **79**, 865 (1997).

⁶L. S. Li and A. P. Alivisatos, *Phys. Rev. Lett.* **90**, 097402 (2003).

⁷T. Nann and J. Schneider, *Chem. Phys. Lett.* **384**, 150 (2004).

⁸M. Shim and P. Guyot-Sionnest, *J. Chem. Phys.* **111**, 6955 (1999).

⁹S. Shanbhag and N. A. Kotov, *J. Phys. Chem. B* **110**, 12211 (2006).

¹⁰K. S. Cho, D. V. Talapin, W. Gaschler, and C. Murray, *J. Am. Chem. Soc.* **127**, 7140 (2005).

¹¹C. A. Leatherdale, W.-K. Woo, F. V. Mikulec, and M. G. Bawendi, *J. Phys. Chem. B* **106**, 7619 (2002).

¹²W. W. Yu, L. Qu, W. Guo, and X. Peng, *Chem. Mater.* **15**, 2854 (2003).

¹³F. van Mourik, M. Chergui, and G. van der Zwan, *J. Phys. Chem. B* **105**, 9715 (2001).

¹⁴A. L. Efros, M. Rosen, M. Kuno, M. Nirmal, D. J. Norris, and M. Bawendi, *Phys. Rev. B* **54**, 4843 (1996).

¹⁵U. E. H. Laheld and G. T. Einevoll, *Phys. Rev. B* **55**, 5184 (1997).

¹⁶A. Al-Salman, A. Tortschanoff, M. Mohamed, D. Tonti, F. van Mourik, and M. Chergui (unpublished).

¹⁷U. Bockelmann and G. Bastard, *Phys. Rev. B* **42**, 8947 (1990).

¹⁸H. Benisty, C. M. Sotomayor-Torres, and C. Weisbuch, *Phys. Rev. B* **44**, 10945 (1991).

¹⁹R. D. Schaller, J. M. Pietryga, S. V. Goupalov, M. A. Petruska, S. A. Ivanov, and V. I. Klimov, *Phys. Rev. Lett.* **95**, 196401 (2005).

²⁰C. Bonati, A. Cannizzo, D. Tonti, A. Tortschanoff, F. van Mourik, and M. Chergui, *Phys. Rev. B* **76**, 033304 (2007).

²¹C. Bonati, M. B. Mohamed, D. Tonti, G. Zgrablic, S. Haacke, F. van Mourik, and M. Chergui, *Phys. Rev. B* **71**, 205317 (2005).